Nucleolar stress in *Drosophila melanogaster*
RNAi-mediated depletion of Nopp140

Allison James, Renford Cindass Jr, Dana Mayer, Stephanie Terhoeve, Courtney Mumphrey and Patrick DiMario*

Department of Biological Sciences; Louisiana State University; Baton Rouge, LA USA

Nucleolar stress results when ribosome biogenesis is disrupted. An excellent example is the human Treacher Collins syndrome in which the loss of the nucleolar chaperone, Treacle, leads to p53-dependent apoptosis in embryonic neural crest cells and ultimately to craniofacial birth defects. Here, we show that depletion of the related nucleolar phosphoprotein, Nopp140, in *Drosophila melanogaster* led to nucleolar stress and eventual lethality when multiple tissues were depleted of Nopp140. We used TEM, immuno-blot analysis and metabolic protein labeling to show the loss of ribosomes. Targeted loss of Nopp140 in larval wing discs caused Caspase-dependent apoptosis which eventually led to defects in the adult wings. These defects were not rescued by a *p53* gene deletion, as the craniofacial defects were in the murine model of TCS, thus suggesting that apoptosis caused by nucleolar stress in *Drosophila* is induced by a p53-independent mechanism. Loss of Nopp140 in larval polyploid midgut cells induced premature autophagy as marked by the accumulation of mCherry-ATG8a into autophagic vesicles. We also found elevated phenoloxidase A3 levels in whole larval lysates and within the hemolymph of Nopp140-depleted larvae vs. hemolymph from parental genotype larvae. Phenoloxidase A3 enrichment was coincident with the appearance of melanotic tumors in the Nopp140-depleted larvae. The occurrence of apoptosis, autophagy and phenoloxidase A3 release to the hemolymph upon nucleolar stress correlated well with the demonstrated activation of Jun N-terminal kinase (JNK) in Nopp140-depleted larvae. We propose that JNK is a central stress response effector that is activated by nucleolar stress in *Drosophila* larvae.

Introduction

The nucleolar phosphoprotein Nopp140[1,2] likely functions as a molecular chaperone for small nucleolar ribonucleoprotein particles (snoRNPs), either in their assembly, transport to the nucleolus from Cajal bodies or in their association with pre-rRNA as these snoRNPs mediate site-specific 2'-*O*-methylation (box C/D snoRNPs) or pseudouridylation (box H/ACA snoRNPs)[3] (reviewed in ref. 4). *Drosophila melanogaster* expresses two isoforms of Nopp140 by alternative slicing.[5] The isoforms are identical up to amino acid residue 584, but then differ in their carboxy termini; one (Nopp140-True) is the canonical ortholog of mammalian Nopp140, while the other (Nopp140-RGG) has a Gly and Arg rich domain common to many RNA-associated proteins. Previously, we used RNAi to target the common 5' end of both splice variant transcripts. *Nopp140* mRNA levels depleted by ≥ 50% caused larval and pupal lethality, while depletions by only ~30% produced viable adults, but with defective legs, wings, thoracic bristles and abdominal cuticles.[6] These adult structures normally derive from larval imaginal discs and histoblasts which presumably maintain high demands for ribosome biogenesis and thus protein synthesis.

Related to Nopp140 in structure and function is Treacle, a nucleolar protein found thus far in vertebrates along with Nopp140. *TCOF1* is the gene on human chromosome 5 that encodes Treacle. Haplo-insufficiencies in *TCOF1* are closely associated with the Treacher Collins-Franceschetti syndrome (TCS), which is marked by craniofacial malformations during fetus development.[7,8] TCS arises from the loss of neural crest cells that normally migrate to populate branchial arches I and II on about day 24 of human embryogenesis.[9] Loss of Treacle in these particular neural crest cells results in abnormal ribosome biogenesis (referred to as nucleolar stress) and thus a loss in protein synthesis leading ultimately to cellular stress and p53-dependent apoptosis.[10] Using the murine system, Jones et al.[10] showed that depleting p53 or blocking p53 function prevented apoptosis in these neural crest cells; they were thus able to rescue the craniofacial abnormalities normally associated with the TCS.

Malformations in adult flies resulting from the partial loss of Nopp140 in *Drosophila* larval progenitor tissues were reminiscent of the human TCS. The first goal of this study was to determine what cell stress responses resulted from the depletion of Nopp140 by RNAi expression in *Drosophila* larval cells leading either to
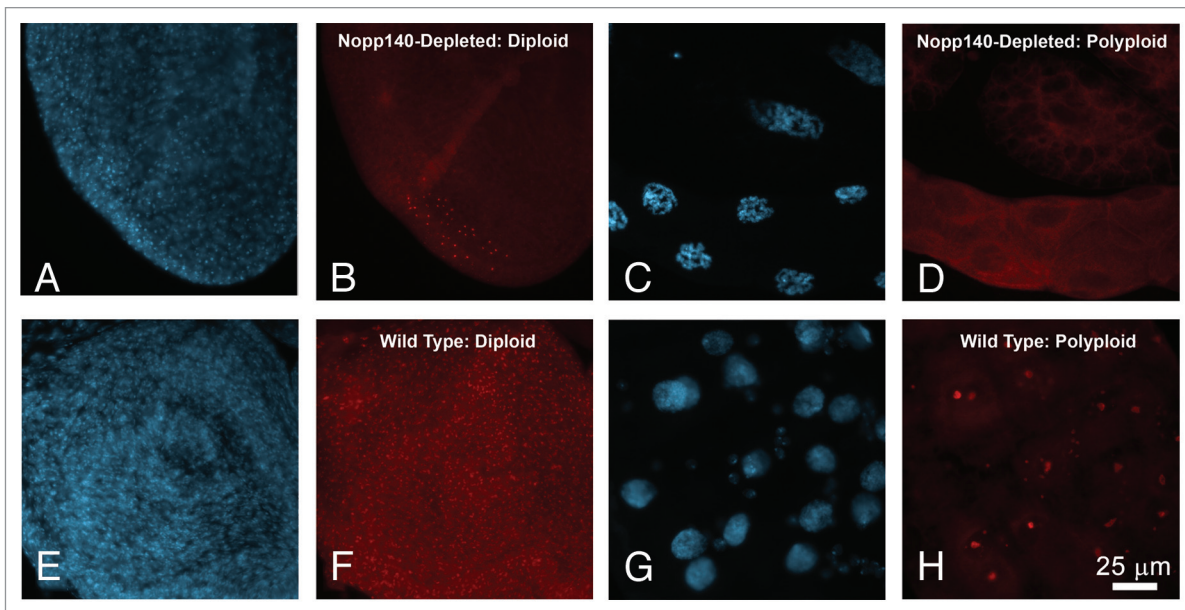
Figure 1. Selective loss of Nopp140 in *Act5C > UAS-C4.2* larvae. Expression of RNAi targeting *Nopp140* transcripts caused depletion of Nopp140 in most tissues as shown by DAPI staining and immuno-fluorescence microscopy using an antibody directed against a unique sequence within the carboxy terminal domain of Nopp140-RGG.[6] (**A and B**) Nucleoli in most small diploid imaginal disc cells from *Act5C > UAS-C4.2* larvae lacked Nopp140-RGG. A few cells retained detectable Nopp140-RGG in their nucleoli (B), due presumably to insufficient RNAi expression in these particular cells. (**C and D**) Nucleoli in giant polyploid cells from *Act5C > UAS-C4.2* larvae also lacked Nopp140-RGG. Polyploid cells lacking Nopp140 contained condensed chromatin.[6] (**E and F**) Nucleoli in most imaginal disc cells from wild type larvae stained with anti-Nopp140-RGG. (**G and H**) Nucleoli in polyploid midgut cells and the smaller imaginal island cells from wild type larvae stained well with the anti-Nopp140-RGG antibody. Scale bar: 25 μm for all images.

lethality or to malformations in adult structures. Apoptosis in larval imaginal disc cells and histoblasts could well explain the morphological defects observed in adult structures. The second goal was to determine if p53 is required for the *Drosophila* nucleolar stress response as it is in the mammalian system. The third goal was to identify principal stress effectors that respond to nucleolar stress responses in *Drosophila*.

Results

We previously used the GAL4 system in *Drosophila* to express RNAi that targeted mRNAs encoding both Nopp140 isoforms.[6] We showed that larvae depleted of *Nopp140* mRNAs to ~50% of wild type levels died in the late third instar larval and pupal stages. Conversely, when reduced Nopp140 transcripts were depleted by only ~30%, the larvae survived to adults, but their wings, legs, thoracic bristles or abdominal cuticles were malformed.[6] Essentially two RNAi-expressing transgenes, *UAS-C3* and *UAS-C4.2*, were used in the following studies. Both effectively reduce Nopp140 levels when induced by GAL4. *UAS-C4.2* maps on the second chromosome and *UAS-C3* maps on the third chromosome; both transgenes reside in the original *UAS-C4* line.[6] For the sake of simplicity, we refer to *UAS-C4.2*, *UAS-C3* or the original *UAS-C4* as *Nopp140-RNAi* in the text, but figure legends differentiate which transgene was actually used in the respective experiments.

Nucleolar stress caused by the loss of Nopp140. Heterozygous *Act5C > Nopp140-RNAi* lacked Nopp140 within most, but not all of their imaginal diploid cells (**Fig. 1A and B**) and polyploid cells

(**Fig. 1C and D**). Polyploid cells lacking Nopp140 condense their chromatin (**Fig. 1C**).[6] These larvae died in the late larval and early pupal stages when reared at 27–28°C. While we used *w^1118* as our wild type control in **Figure 1E–H,** homozygous parental larvae develop normally (they are viable and fertile) with no detectable loss of Nopp140 in their tissues.

We compared tissues from *Act5C > Nopp140-RNAi* larvae to the same tissues from wild type (*w^1118*) or parental type larvae by transmission electron microscopy, immuno-blot analysis and metabolic protein labeling to confirm that ribosome synthesis was disrupted due to Nopp140 depletion (i.e., nucleolar stress). A diploid cell from an *Act5C > Nopp140-RNAi* larval wing disc (**Fig. 2A**) contained some rough endoplasmic reticulum, but the number of free ribosomes in the cytosol was greatly reduced compared with that in the wild type disc cell (**Fig. 2B**). In addition, the nuclei (Nu) in the *Act5C > Nopp140-RNAi* diploid cells contained numerous virus-like particles (arrow in **Fig. 2A**). These particles likely arise from *copia* retrotransposons[11] that can be induced by environmental stress,[12] aging[13] or perturbations in poly(ADP-ribose) polymerase.[14] In preparing tissues for TEM analysis, we noted the small size of the imaginal discs isolated from *Act5C > Nopp140-RNAi* larvae. We have yet to determine if reduced disc size is due to smaller cells or failure to produce sufficient cell numbers. A polyploid midgut cell from an *Act5C > Nopp140-RNAi* larva (**Fig. 2C**) contained relatively very few ribosomes as compared with the same cell type from a wild type larva (**Fig. 2D**). Again, the presence of virus-like bodies the nucleus (arrow in **Fig. 2C**) indicated these Nopp140-depleted polyploid cells were under stress. While *Act5C > Nopp140-RNAi* imaginal
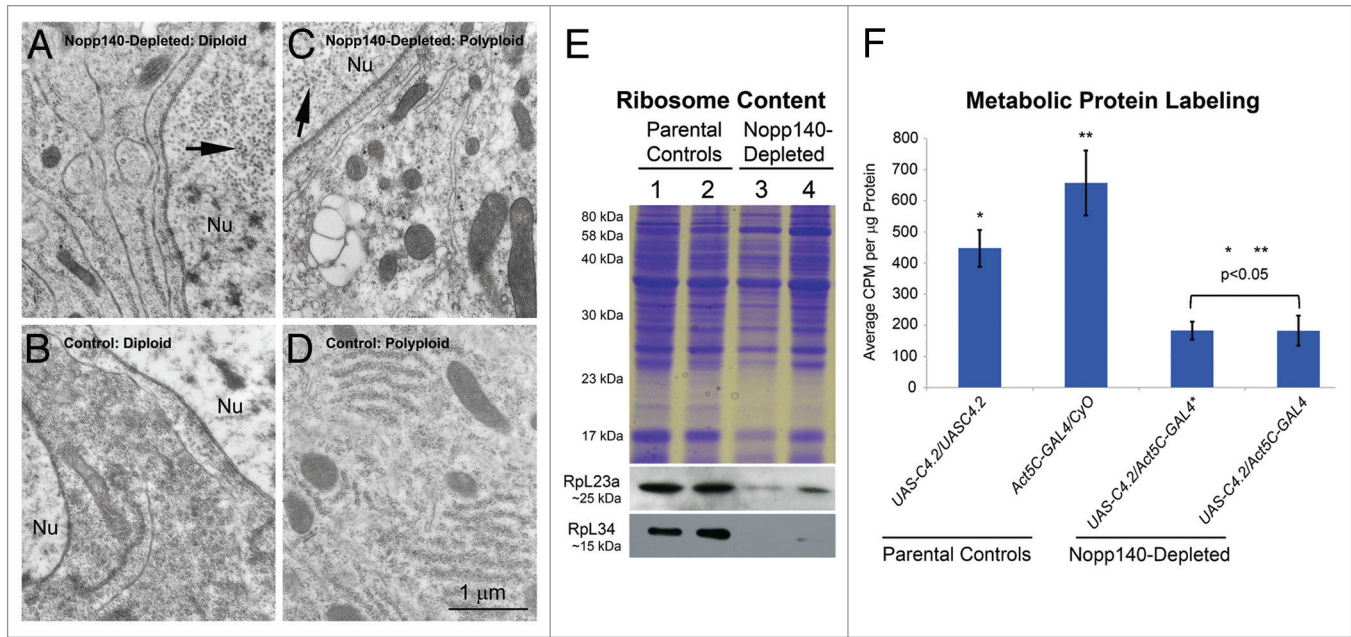
Figure 2. TEM, immuno-blot analysis and metabolic protein labeling demonstrate loss of ribosomes and protein synthesis. (**A–D**) Separate tissues were isolated by hand and prepared for TEM analysis. Imaginal wing disc cells from *Act5C > UAS-C4.2* larvae (**A**) contained fewer ribosomes as compared with similar cells from wild type (*w[1118]*) larvae (**B**). Polyploid midgut cells from *Act5C > UAS-C4.2* larvae (**C**) contained far fewer ribosomes than did similar, identical cells from wild type (*w[1118]*) larvae (**D**). Nuclei (Nu) in *Act5C > UAS-C4.2* larvae (panels A and C) contained numerous *copia* virus-like particles indicating stress. Scale bar: 1 μm for all TEM images. (**E**) Specific antibodies showed a loss of RpL23a and RpL34 in lysates from *Act5C > UAS-C4.2* larvae compared with parental type larvae. Lane 1: homozygous *UAS-C4.2* parental lysate; Lane 2: heterozygous *Act5C-GAL4/CyO-GFP* parental lysate; Lane 3: RNAi-expressing *UAS-C4.2/Act5C-GAL4* lysate; Lane 4: a separate RNAi-expressing *UAS-C4.2/Act5C-GAL4* lysate. (**F**) Metabolic protein labeling was significantly reduced in Nopp140-RNAi-expressing *UAS-C4.2/Act5C-GAL4* larvae compared with larval parental controls. The entire experiment was repeated three times. Absorbance values were determined in triplicate. Graphs were assembled using Microsoft Excel; two-tailed P values were equated using t-Test analysis (two sample assuming unequal variances).

discs failed to grow, brains from these larvae appeared normal in size; the brain cells showed normal levels of cytoplasmic ribosomes, and their nuclei were clear of virus-like bodies (image not shown). This was surprising since the endogenous *Act5C* gene is normally expressed at high levels in the larval central nervous system, and we expected the *Act5C-GAL4* transgene would be similarly expressed. One possibility is that Nopp140 expression levels may be sufficiently high in the larval central nervous system[48] (see http://flybase.org/reports/FBgn0037137.html) such that Nopp140-RNAi expression cannot effectively deplete enough Nopp140 to disrupt ribosome synthesis.

By immuno-blot analysis (**Fig. 2E**), we saw a loss of ribosomal proteins L23A and L34 in third instar *Act5C > Nopp140-RNAi* larvae (lanes 3 and 4) compared with the two respective parental larval types (lanes 1 and 2). We note, however, that younger *Act5C > Nopp140-RNAi* larvae that had yet to show obvious defects such as melanotic tumors (see below) contained near normal levels of ribosomal proteins (lane not shown). These younger larvae likely maintained sufficient quantities of maternal Nopp140 and ribosomes that dwindle as these larvae advance further into the third instar stage.

To verify the effects of ribosome loss in third instar larvae, we compared metabolic protein labeling in parental control larvae vs. *Act5C > Nopp140-RNAi* larvae depleted for Nopp140. The loss of Nopp140, leading to the loss of ribosomes, caused a

reduction in protein synthesis to ≤ 40% (**Fig. 2F**). In this assay, we analyzed two separate samples of *Act5C > Nopp140-RNAi*. One sample (*) was older with a greater number of melanotic masses compared with the other, yet we saw similar protein labeling profiles in the two samples. We conclude from the various assays in **Figure 2** that third instar *Act5C > Nopp140-RNAi* larvae had a pronounced loss of ribosomes and thus protein synthesis, and this resulted in lethality by the late third larval instar-early pupal stages.

Selective depletion of Nopp140 in larval wing discs. To assess the loss of Nopp140 without inducing lethality, we used the larval wing disc driver, *A9-GAL4,* on the *X* chromosome to induce the *Nopp140-RNAi* gene (*UAS-C4.2* on the second chromosome) (*A9 > UAS-C4.2*). We set up the cross such that all male progeny displayed normal wings. Conversely, female progeny (*A9 > Nopp140-RNAi*) expressed RNAi in their larval wing discs, which eventually led to malformed adult wings. The wing phenotype in these females varied from a relatively mild upward curl along the anterior and posterior edges of the wing to severely shriveled (vestigial-like) wings (see **Table 1**). Large fluid-filled blisters were common in the wings of newly eclosed females. Their wings were left badly malformed as the blisters receded over time. **Table 1** compares the frequency of the severe wing phenotype to that of the less severe curled wing phenotype. While all the male progeny had normal wings, 47% of the *A9 >*

Table 1. X and/or Y chromosome, second chromosome and third chromosome designations are separated by semi-colons

Progeny Phenotypes \ Progeny Genotypes		w/Y; UAS-C4.2/+; +/+ ♂♂	A9/w⁻; UAS-C4.2/+; +/+ ♀♀	w/Y; UAS-C4.2/+; Δp53/Δp53 ♂♂	A9/w⁻; UAS-C4.2/+; Δp53/Δp53 ♀♀
Normal wings		100%	0%	100%	0%
Mild wing edge curl		0%	47%	0%	42%
Severe wing malformation		0%	53%	0%	58%
Number of Flies Scored		270	172	143	178

Male larvae (*w^1118^/Y*) lacked the *A9-GAL4* driver and therefore did not express RNAi from *UAS-C4.2* on their second chromosome. Female larvae (*A9/w^1118^*) expressed RNAi to deplete Nopp140 in their wing discs. Two crosses were performed, with (+) and without (Δ) the *p53* gene on the third chromosome. Abnormal wing phenotypes appeared in only the females as either a mild wing edge curl or a more severe vestigial-like (shriveled) wing. Phenotype frequencies were comparable with or without the *p53* gene.

Nopp140-RNAi females showed wings with the mild defect, and the remaining 53% showed the severe defect. None of the females had normal wings. We conclude that *A9 > Nopp140-RNAi* provides a non-lethal phenotype that we can score to access nucleolar stress in diploid imaginal (progenitor) wing disc cells.

TCS arises in mammals when specialized embryonic neural crest cells undergo apoptosis due to the loss of Treacle.[10] To determine if nucleolar stress caused by the loss of Nopp140 in *Drosophila* wing discs also induces apoptosis, we reversed the original cross for **Table 1** such that homozygous *A9-GAL4* driver females were crossed to males homozygous for *Nopp140-RNAi*. All larval progeny from this cross expressed Nopp140-RNAi in their wing discs. We probed these wing discs with anti-cleaved Caspase 3 (Asp175) from Cell Signaling Technology. Although the precise antigen remains unknown, this particular antibody provides a good marker for Caspase-9-like DRONC activity in apoptotic *Drosophila* cells.[15] A wing disc from an *A9 > Nopp140-RNAi* larva was heavily labeled by anti-Caspase (**Fig. 3A–C**). Higher magnification showed that the apoptotic cells contained condensed chromatin within their nuclei (**Fig. 3D**) and that anti-Caspase 3 labeled the cytoplasm (**Fig. 3E**) as expected. Wing discs from wild type larvae (*w^1118^*) showed minimal anti-Caspase labeling (**Fig. 3F–H**). Therefore, as with the loss of Treacle in mammalian neural crest cells, selective loss of Nopp140 in *Drosophila* imaginal wing disc cells induced apoptosis leading to malformed wings in adult flies.

Apoptosis induced by nucleolar stress in *Drosophila* is p53-independent. Jones et al.[10] showed that apoptosis induced by nucleolar stress in mouse embryonic neural crest cells was p53-dependent. The deletion of the mouse *p53* gene or chemical inactivation of p53 suppressed this apoptosis, reducing the severity of phenotypes typically associated with TCS. To test if apoptosis in *Drosophila* imaginal wing discs resulting from depletion of Nopp140 is p53-dependent, we repeated the original cross

described in **Table 1** such that only female progeny would display wing defects, but this time the two parental types (the *A9-GAL4* driver and the Nopp140-RNAi-expressing lines) were homozygous for the *p53* gene deletion (*p53^[5A-1-4]^*) on the third chromosome (referred to simply as *p53Δ*). This deletion was originally described by Rong et al.[16]; homozygous deletion flies are viable and fertile, but they display reduced apoptosis in response to DNA damage caused by ionizing radiation.[17-19]

Genomic PCRs verified that the modified parental lines were in fact deleted for *p53* (**Fig. 4A**). The wild type *p53* gene in *w^1118^* flies produced the expected 7.3 kbp PCR product (lane 1), while the modified *A9-GAL4* driver (lane 2), the original *p53Δ/p53Δ* stock from the Bloomington Stock Center (lane 3) and the *Nopp140-RNAi* line (lane 4) produced the expected 4.0 kbp product indicating homozygous deletion of the *p53* gene (see Flybase, http://flybase.org/reports/FBrf0151688.html for descriptions of the expected PCR products). Thus, all *A9 > Nopp140-RNAi* progeny from this second cross should be homozygous deficient for the *p53* gene. While the male progeny from this cross showed normal wings as expected (**Fig. 4B**, left wing), all female progeny again displayed malformed wings (**Fig. 4B**, right wing). **Table 1** again summarizes the results: of the female progeny obtained, 42% displayed the less severe curled wing edge phenotype, while 58% showed the more severe shriveled wing phenotype (**Table 1**). This compares well to 47% and 53%, respectively, for those female progeny that were homozygous for the wild type *p53* gene. We note that variability in wing phenotype in both crosses (with and without *p53*) may be caused to slight temperature fluctuations affecting GAL4-mediated induction of *UAS*-transgenes. To minimize this effect, all crosses were performed at 27–28°C.

We again reversed the cross such that all progeny were *A9 > Nopp140-RNAi; p53Δ/p53Δ*. These larvae also showed apoptosis in wing discs by anti-Caspase 3 labeling (**Fig. 4C and D**). We performed these crosses several times to be certain that the
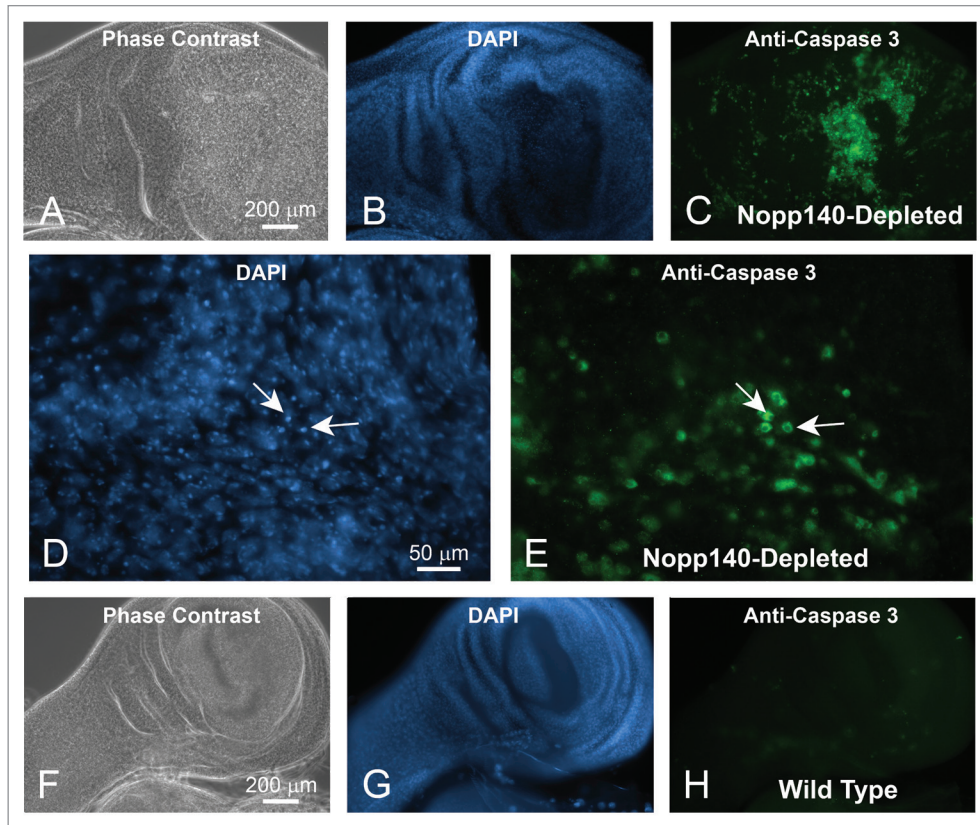
Figure 3. Loss of Nopp140 in imaginal wing discs of *A9 > UAS-C4.2* larvae resulted in apoptosis. Phase contrast (**A**) and DAPI staining (**B**) of a wing disc isolated from an *A9 > UAS-C4.2* larva. (**C**) The wing disc stained heavily with anti-Caspase 3 indicating apoptosis. (**D and E**) Higher magnification of panels (**B and C**) showed anti-Caspase 3 staining in the cytoplasm as expected. Cells with copious anti-Caspase 3 labeling showed condensed chromatin by DAPI staining (arrows). (**F–H**) Wing discs from control (*w^1118^*) larvae were probed with anti-Caspase 3 antibody. They showed minimal background labeling.

presence or absence of p53 had no effect on wing malformations due to Nopp140 depletion. The combined data in **Table 1** indicates that there were no appreciable differences in the abnormal wing phenotypes due to Nopp140 depletion when *p53* was present or deleted. We conclude, therefore, that larvae selectively depleted for Nopp140 in their wing discs induce apoptosis in these discs, but in a p53-independent manner.

Autophagy in larval polyploidy midgut cells depleted of Nopp140. In earlier studies to examine the loss of Nucleostemin I in *Drosophila* larvae, we observed by TEM premature autophagy in larval polyploid midgut cells.[20] Here, we ectopically co-expressed mCherry-ATG8a[21] to determine if excessive autophagy occurred in midgut cells of Nopp140-depleted (*da > Nopp140-RNAi; UAS-mCherry-ATG8a*) third instar larvae. We first expressed mCherry-ATG8a in the midgut of a second instar larva using the *da-GAL4* driver, but in an otherwise wild type background; mCherry-ATG8a distributed diffusely throughout these midgut cells (**Fig. 5A**). As a positive control for autophagy, we starved similar second instar larvae to induce autophagy.[22] As expected, mCherry-ATG8 aggregated into vesicles within the cytoplasm of these midgut polyploid cells (**Fig. 5B**). We interpret the appearance of these vesicles as autophagosomes and lysosomes.[23] Similar vesicles with mCherry-ATG8 appeared prematurely and in great

abundance in the midgut of Nopp140-depleted larvae (*da-GAL4 > Nopp140-RNAi; UAS-mCherry-ATG8a*) (**Fig. 5C**). Thus, the loss of Nopp140 and nucleolar function induces premature autophagy in the polyploid midgut cells.

Accumulation of phenoloxidase A3 in response to Nopp140 depletion. Coomassie-stained SDS-gels showed an abundant 70 kDa protein in whole lysates of *Act5C > Nopp140-RNAi* larvae vs. parental control larvae (**Fig. 6A**). At first, we thought the accumulated protein was a classic heat shock protein (Hsp70) or perhaps a heat shock cognate protein (Hsc70) that was induced upon nucleolar stress. However, antibodies against Hsp70 and Hsc70 failed to show significant accumulations of either protein in the Nopp140-depleted larvae. LC-MS/MS finally identified the protein as phenoloxidase A3 encoded by *PO45* (conceptual gene *CG8193)* in *Drosophila melanogaster*.

Phenoloxidases in *Drosophila* are released into the hemolymph from circulating crystal cells, usually as part of an innate immune response to parasitic infection. Upon infection, the phenoloxidases convert phenols to quinones that polymerize to form melanin aggregates that then encapsulate the parasite.[24] To test if phenoloxidases were released to the hemolymph of Nopp140-depleted larvae, we isolated larval serum proteins,[25] resolved them on native polyacrylamide gels and then either stained the gels
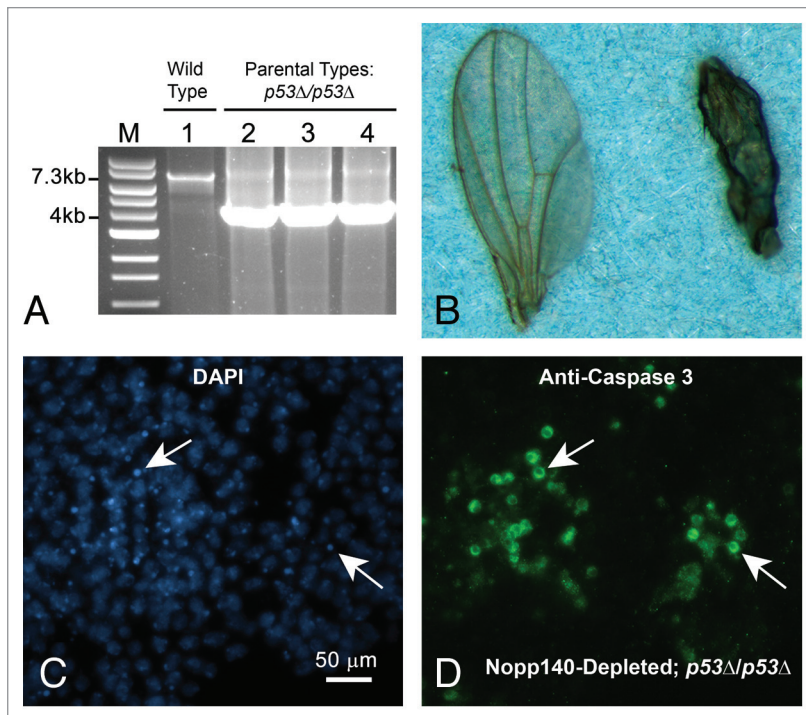
Figure 4. Verifying the *p53* gene deletion in parental stocks and establishing p53-independent apoptosis in Nopp140-depleted wing discs. (**A**) The *p53* gene deletion was verified using genomic PCR. The 7.3 kb band denotes presence of the wild type p53 gene while the 4.0 kb band denotes its deletion. Tested genotypes were: *w[1118]* stock (wild type) (lane 1), *A9-GAL4/A9-GAL4*; +/+; *p53Δ/p53Δ* (the GAL4 driver*)* (lane 2), the original *p53Δ/p53Δ* stock (Bloomington 6815) (lane 3), *w[1118]/w[1118]*; *UAS-C4.2/UAS-C4.2*; *p53Δ/p53Δ* (RNAi) (lane 4). (**B**) The cross reported in **Table 1** was repeated using the *A9-GAL4 and UAS-C4.2* lines that were homozygous for *p53Δ*. Adult male progeny (*w[1118]/Y*; *UAS-C4.2/+*; *p53Δ/p53Δ*) again produced normal wings (left wing), while female progeny (*A9-GAL4/w[1118]*; *UAS-C4.2/+*; *p53Δ/p53Δ*) expressed RNAi to deplete Nopp140 and again displayed malformed wings (right wing). (**C and D**) Apoptosis was evident in the larval wing discs of *A9 > UAS-C4.2*; *p53Δ/p53Δ* larvae as shown by anti-Caspase 3 labeling within the cytoplasm. White arrows point to corresponding nuclei containing condensed chromatin.

with Coomassie blue (**Fig. 6B**) or stained the gels for phenoloxidase activity using tyrosine as a substrate[26] (**Fig. 6C**). Compared with parental types, *Act5C > Nopp140-RNAi* larvae showed greater amounts of phenoloxidase in their hemolymph, indicating another phenotype associated with the loss of nucleolar function. In collecting the *Act5C > Nopp140-RNAi* larvae, we purposely pooled larvae with numerous melanotic masses. These larvae are designated with an asterisk in **Figure 6**, and they showed more phenoloxidase in their hemolymph than did *Act5C > Nopp140-RNAi* larvae with only a few melanotic masses.

We noted previously the accumulation of melanotic masses (tumors) in Nopp140-depleted larvae and pupae.[6] These masses seem to arise preferentially in the midgut (**Fig. 6D**), but we also found melanotic masses scattered throughout the larva; for example, **Figure 6E** shows melanotic masses at the ends of the dorsal arms of the pharyngeal sclerite. The observed rise in phenoloxidase abundance in whole lysates and its accumulation in the hemolymph correlate well with the appearance of melanotic masses in Nopp140-depleted larvae.

JNK and pro-apoptotic Hid are activated in response to nucleolar failure. Thus far we have documented three stress response phenotypes that arise due to the loss of nucleolar function: apoptosis in imaginal wing discs, autophagy in polyploid midgut cells and the formation of melanotic masses due to the release of phenoloxidase from crystal cells. JNK (also known as the stress-activated protein kinase, SAPK) is a principal cell stress response effector[27,28] that could link all three phenotypes. Activated *Drosophila* JNK (also referred to as basket) is known to induce apoptosis by activating *Hid*[29] and autophagy by inducing *dFoxo*.[30,31] Activated JNK also induces the rupture of crystal cells to release phenoloxidases.[32] Therefore, we tested if *Drosophila* JNK is activated in Nopp140-depleted larvae (**Fig. 7B**). Activation of human JNK is marked by the phosphorylation of residues Thr183 and Tyr185. These residues are conserved in the one isoform of JNK expressed in *D. melanogaster*. The rabbit monoclonal antibody 81E11 from Cell Signaling cross reacted well with activated *Drosophila* JNK on immuno-blots (**Fig. 7B**). Whole lysates from *Act5C > Nopp140-RNAi* larvae showed an elevated level of activated JNK vs. lysates from parental controls. We conclude that activated JNK accumulates in Nopp140-depleted larvae.

The anti-pJNK immuno-blot (**Fig. 7B**) showed two bands in some lysate preparations from both parental types and from the Nopp140-depleted larvae, while we saw only the higher molecular weight band in other separately prepared lysates. At this time we have no clear explanation for the appearance of the bottom band other than partial proteolysis.

In their model of p53-independent apoptosis in *Drosophila*, McNamee and Brodsky[33] proposed that JNK induces Hid protein expression that then induces apoptosis. To test if *Hid* was induced, we probed the same lysates used in **Figure 7B** with a rabbit polyclonal antibody directed against *Drosophila* Hid.[34] We found Hid levels notably increased in *Actin5C > Nopp140-RNAi* larvae vs. parental controls (**Fig. 7A**).

Discussion

The human TCS results from mutations in the *TCOF1* gene which encodes the nucleolar phosphoprotein, Treacle. Subsets of embryonic neural crest cells are particularly sensitive to the loss of Treacle, a nucleolar chaperone for ribosome biosynthesis. These cells normally migrate to populate embryonic branchial arches I and II that then give rise to adult craniofacial structures. Without Treacle, these neural crest cells fail to meet a relatively high threshold requirement for functional ribosomes. As a result these cells are stressed and undergo p53-dependent apoptosis. Their loss ultimately leads to the craniofacial malformations associated with the TCS. Jones et al.[10] could alleviate the syndrome by blocking p53
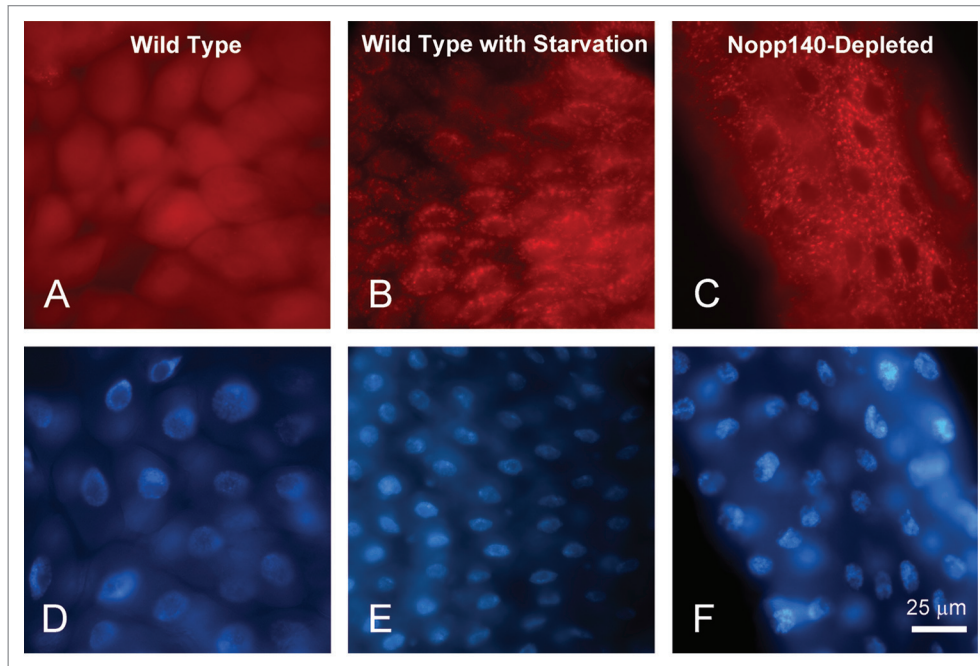
Figure 5. Autophagy was prominent in larval polyploid cells depleted for Nopp140. (**A and D**) *da > mCherry-ATG8* in a wild type background. Labeling remained diffuse throughout the cell. (**B and E**) As a positive control for autophagy, similar *da > mCherry-ATG8a* larvae were starved of amino acids. The accumulation of mCherry-ATG8a into autophagosomes and lysosomes (red speckling in the cytoplasm) indicated autophagy as expected due to starvation. (**C and F**) Well fed *da > UAS-C4.2; mCherry-ATG8a* larvae displayed similar accumulations of mCherry-ATG8a into cytoplasmic vesicles within their midgut cells indicating premature autophagy in response to the loss of Nopp140.

function either by a *p53* gene deletion or by a specific p53 protein inhibitor.

Vertebrate Nopp140 and Treacle are related in structure and function.[4] Both proteins are over 100 kDa in size, both contain LisH dimerization motifs in their N-terminal region, and both proteins contain a large central domain consisting of alternating acidic and basic motifs with similar amino acid compositions; the acidic motifs are rich in Glu, Asp and phospho-Ser, while the basic motifs are rich in Lys and Pro. Both proteins are believed to function as chaperones for snoRNP complexes as these complexes direct site-specific methylation and pseudouridylation of pre-rRNA within the dense fibrillar regions of eukaryotic nucleoli. While most snoRNAs appear to be non-essential when individually deleted, failure to collectively modify pre-rRNA by the loss of a snoRNP chaperone would likely produce defective or partially functional ribosomes in all cells. Embryonic progenitor cells with high demands for protein synthesis would be most susceptible to the loss of functional ribosomes. Loss of these cells would lead to lethality or developmental defects. Thus Treacle and Nopp140 are required for normal development. Despite their multiple similarities, Nopp140 and Treacle differ in their carboxy termini, suggesting that each protein maintains its own unique interactions and functions. Interestingly, while *Drosophila* expresses two isoforms of Nopp140 by alternative splicing,[5] *Drosophila* lacks a Treacle ortholog.

We showed that larval cells depleted for Nopp140 undergo a disruption in ribosome biosynthesis (nucleolar stress). Larval tissues expressing *Nopp140-RNAi*, both diploid and polyploid,

have fewer ribosomes than wild type (**Fig. 2A–D**). These larvae also have reduced amounts of ribosomal proteins L23 and L34 (**Fig. 2E**). Metabolic labeling verified these findings, revealing that Nopp140-depleted larvae synthesize significantly reduced amounts of protein (≤ 40%) compared with parental controls (**Fig. 2F**). As larval tissues develop, maternally supplied ribosomes and Nopp140 diminish, and cells expressing *Nopp140-RNAi* are unable to supply either functional ribosomes and/or sufficient protein synthesis. This nucleolar stress thus leads to distinctive cell death pathways.

Here we showed that the loss of *Drosophila* Nopp140 specifically in imaginal wing disc cells lead to apoptosis and impaired wing development, analogous to the loss of Treacle in embryonic neural crest cells. However, while Jones et al.[10] rescued the TCS in mice by employing a *p53* gene deletion, the similar rescue failed in *Drosophila* as apoptosis occurred in the absence of the *p53* gene (**Fig. 3**). Induction of apoptosis in the absence of p53 has been well documented in *Drosophila*.[18,33]

Besides apoptosis, we documented a strong and premature induction of autophagy in larval midgut polyploid cells that were depleted for Nopp140 (**Fig. 5C**). As with apoptosis, JNK activation is reportedly linked to autophagy induction[22] by way of the downstream activation of dFoxo.[30] We note, however, that this stress-induced autophagy is in contrast to a JNK-independent induction of autophagy that normally occurs during development or in response to starvation resulting in the inhibition of Tor signaling.[22,23]

We also showed that formation of excess melanotic masses in Nopp140-depleted larvae was coincident with the accumulation
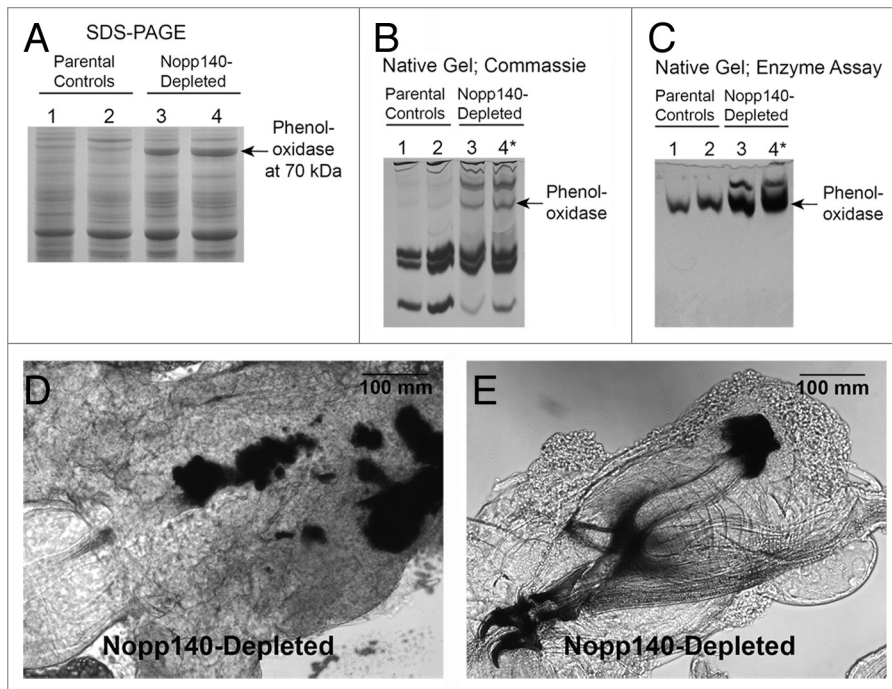
Figure 6. Phenoloxidase A3 accumulated in Nopp140-depleted larvae. (**A**) Whole larval lysates from parental control larvae (*Act5C-GAL4/CyO*, lane 1; homozygous *UAS-C4.2*, lane 2) were compared with those from Nopp140-depleted larvae (*UAS-C4.2/Act5C-GAL4*, lane 3; *UAS-C4/Act5C-GAL4*, lane 4). *UAS-C4* is the original stock containing *UAS-C4.2* on the 2nd chromosome and *UAS-C3* on the 3rd chromosome. The prominent 70 kDa protein in the lysates of Nopp140-depleted larvae (arrow) was identified by LC-MS/MS as phenoloxidase A3. (**B**) Hemolymph proteins were resolved on a native polyacrylamide gel and stained with Coomassie blue. Parental control larvae were homozygous *UAS-C4.2* (lane 1) and *Act5C/CyO-GAL4* (lane 2). Nopp140-RNAi-expressing *UAS-C4.2/Act5C-GAL4* larvae (lane 3) with only a few melanotic masses were compared with similar *UAS-C4.2/Act5C-GAL4** larvae (lane 4) that had excess melanotic masses. (**C**) A native gel similar to that shown in panel (**B**) but stained for phenoloxidase activity using tyrosine as substrate. Arrows in (**B and C**) mark the position of the most prominent phenoloxidase activity. (**D**) Melanotic masses were found mostly in the midgut of *Act5C > UAS-C4.2* larvae. (**E**) Melanotic masses also occurred at other sites within *Act5C > UAS-C4.2* larvae. This large mass accumulated at the tips of the dorsal arms of the pharyngeal sclerite.

of phenoloxidase A3 both in whole larval lysates (**Fig. 6A**) and in the larval hemolymph (**Fig. 6B and C**). While phenoloxidases are normally synthesized and stored in crystal cells, they are not secreted in a typical secretory pathway; rather, crystal cells rupture in a JNK-dependent manner releasing the phenoloxidases to the hemolymph.[24,32] How Nopp140-depleted larvae synthesize excess amounts of phenoloxidase when nucleolar function (ribosome biosynthesis) is impaired remains a perplexing question. Since the Nopp140-depleted larvae are developmentally delayed, we speculate that phenoloxidase A3 may simply amass in abundance over time despite a slow rate of protein synthesis as compared with wild type larvae. This could explain the excess accumulations of phenoloxidase in whole larval lysates as shown by Coomassie-stained gels (**Fig. 6A**). The activation of JNK in the Nopp140-depeleted larvae may then release the phenoloxidase to the hemolymph as shown in the hemolymph enrichments (**Fig. 6B and C**).

Many of the melanotic masses we saw seemed to reside within non-hematopoietic tissues such as the midgut, trachea and salivary glands.[35] One possibility suggested by Bidla et al.[32] is that apoptosis followed by secondary necrosis triggers formation of melanotic masses. If so, we would expect to see the formation of multiple melanotic masses at non-hematopoietic sites undergoing heavy apoptosis and secondary necrosis.

Nucleolar stress in *Drosophila* vs. mammals. Our working hypothesis is that depletion of Nopp140 in *Drosophila* cells disrupts normal ribosome biogenesis, a term now referred to as "nucleolar stress."[36,37] Studies on nucleolar stress in mammalian cells have focused primarily on the nucleolar protein ARF (p19[ARF] in mice, p14[ARF] in humans), its interactions with MDM2 which is the E3 ubiquitin ligase for p53 and the role that nucleolar protein B23 plays in sequestering ARF to the nucleolus.[37] Upon stress in mammalian cells, ARF indirectly activates p53 by interacting with MDM2 to suppress its ubiquitylation of p53. Under these conditions, p53 accumulates and activates genes necessary for cell cycle arrest, senescence or apoptosis. Interestingly, *Drosophila* lacks identifiable ARF, MDM2 and B23. Thus nucleolar stress in *Drosophila* likely plays out by an alternative mechanism.

From our work, JNK appears to be a common link between *Hid* (apoptosis), *dFoxo* (autophagy)[22,30] and the release of phenoloxidases from crystal cells as these cells rupture in JNK-dependent manner.[32] We showed by immuno-blot analysis that Hid rises (**Fig. 7A**) coincidently with activated JNK (**Fig. 7B**) in Nopp140-depleted larvae. While JNK activation has been reported to be delayed in the p53-independent mechanism,[18,38] once activated, JNK is thought to induce *Hid* expression and thus apoptosis.[33] While we have yet to assess the abundance and activities of dFoxo and dFos in the Nopp140-depleted larvae, others have shown that Hid induction results from JNK activation via these two transcription factors.[29,39] From the combined evidence, we propose that JNK is a central effector activated in response to perturbations in *Drosophila* ribosome biogenesis.

JNK is a member of the MAP kinase superfamily, and while mammals express multiple forms of JNK, *Drosophila melanogaster* expresses only one version of JNK (basket). Precisely how *Drosophila* JNK is activated in response to nucleolar failure remains unknown. As a clue, Moreno et al.[40] showed that JNK signaling is required for the apoptotic elimination of slowly proliferating *Minute^{-/+}* cells in larval wing discs where *Minute[-]* is a dominant, haplo-insufficient mutation in a gene encoding a ribosomal protein.[41] McNamee and Brodsky[33] proposed that gene haplo-insufficiencies in these same ribosomal protein genes could induce expression of *brinker* (*brk*) which encodes a transcription factor in larval wing discs, and that *brk* is sufficient to activate JNK, thus leading to apoptosis. Also

upstream of *Drosophila* JNK are at least two JNKKs (Hemipterous and MKK4) and several JNKKKs. Puckered is the *Drosophila* protein phosphatase that is also induced by JNK to deactivate JNK in a negative feedback loop. How Hemipterous and Puckered are regulated upon nucleolar stress in *Drosophila* remains unknown. Our future efforts in linking nucleolar stress to JNK activation will examine the expression levels of *brk*, *hemipterous* and *puckered*.

Finally, JNK signaling has been implicated in direct nucleolar function. For example, mammalian JNK2 phosphorylates the RNA polymerase I transcription factor, TIF-IA, to downregulate rRNA synthesis.[42] JNK activity was also required for the release of B23 and p19[ARF] from mammalian nucleoli upon UV radiation (DNA-damage).[43] Conversely, Mialon et al.[44] showed that upon genetic or chemical inhibition of JNK signaling, the mammalian nucleolar RNA helicase, DDX21, is partially redistributed to the nucleoplasm and that rRNA processing is inhibited. Their observation suggests that besides stress-induced JNK-activation, JNK signaling maintains homeostasis for the nucleolus in non-stressed cells. Thus the effects of activated JNK on the localization of *Drosophila* nucleolar components during normal cell growth and upon stress remain largely unknown, but subject for future investigation.

Materials and Methods

Fly lines. Fly lines expressing short hairpin RNA specific for the common 5' end of mRNAs that encode the two Nopp140 isoforms were *P{w[+mC] = UAS-Nopp140.dsRNA}^C3* and *P{w[+mC] = UAS-Nopp140.dsRNA}^C4.2* as described previously.[6] Here we refer to them simply as *UAS-C3* and *UAS-C4.2*. *UAS-C3* resides on the third chromosome. The original *UAS-C4* line contained two RNAi-expressing transgenes: one on the second chromosome and the other on the third chromosome. The transgene on the third chromosome is *UAS-C3*. We isolated the second chromosome from *UAS-C4* and refer to the resulting line as *UAS-C4.2*. Both *UAS-C3* and *UAS-C4.2* lines are homozygous viable and fertile. The *P{UAS-mCherry-Atg8a}* line, D169 (third chromosome), was a kind gift from Thomas Neufeld.[21] Four additional lines came from the Bloomington *Drosophila* Stock Center; stock 6815 is a deletion for the *p53* gene (*p53^[5A-1-4]*).[16] We refer to this deletion simply as *p53Δ* throughout this report. GAL4 driver lines included *P{w[+mC] = Actin5C-GAL4}25FO1/CyO* (stock 4414, referred to simply as *Act5C-GAL4*), the homozygous *daughterless-GAL4* line on the third chromosome (stock 8641, referred to as da-GAL4) and the wing disc-specific *P{w[+m*] = GAL4}A9* on the *X* chromosome (stock 8761, referred to here as *A9-GAL4*). A9-GAL4 expresses GAL4 strongly in larval wing and haltere discs.[45] We previously used the *w^1118* line (Bloomington stock 3605) to construct our RNAi-expressing transgenic lines,[6] and we use it here as our "wild type" control. All stocks were reared at 22–24°C on standard *Drosophila* medium. Genetic crosses using GAL4 drivers were kept at 27–28°C.

Genomic PCR to verify p53Δ. Genomic DNA from adult flies was prepared according to E. Jay Rehm of the Berkeley Drosophila Genome Project
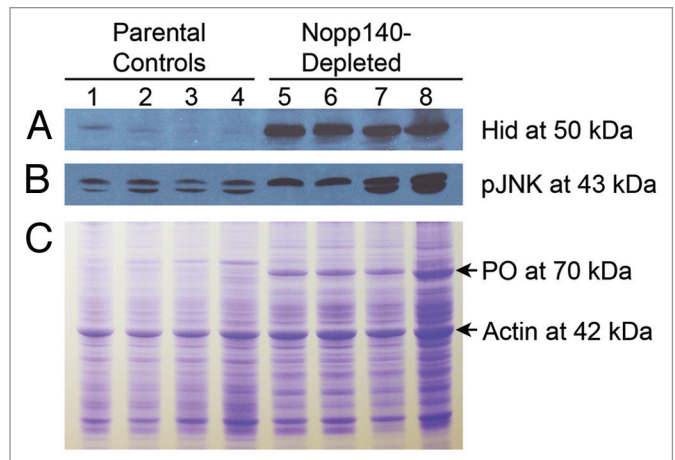
Figure 7. Pro-apoptotic Hid and activated JNK were both upregulated in Nopp140-depleted larvae. (**A**) An immuno-blot containing lysates from parental control larvae (lanes 1–4) and *Act5C > Nopp140-RNAi* larvae (lanes 5–8) was probed with rabbit anti-Hid.[34] Hid at ~50 kDa was substantially increased in the Nopp140-depleted larvae as compared with parental larvae. Lane 1: homozygous *UAS-C4.2*; Lane 2: *Act5C-GAL4/CyO*; Lane 3: *Act5C-GAL4/+*; Lane 4: *CyO-GFP/+*, Lanes 5 and 7: *UAS-C4.2/Act5C-GAL4*; Lanes 6 and 8: *UAS-C4/Act5C-GAL4*. *UAS-C4* is the original transgenic stock that contains *UAS-C4.2* on the 2nd chromosome and *UAS-C3* on the third chromosome. (**B**) A companion blot with the same lysates was probed with rabbit monoclonal antibody 81E11 (Cell Signaling #4668) directed against phospho-JNK at 43 kDa. (**C**) Equal amounts of the same lysates as used in panels A and B were resolved on a Coomassie-stained SDS-gel. Phenoloxidase A3 (PO) is at 70 kDa.

(http://www.fruitfly.org/about/methods/inverse.pcr.html). Primers for verifying the *p53* gene deletion (*p53^[5A-1-4]*) were described by K. Golic in a reference report to FlyBase (http://flybase.org/reports/FBrf0151688.html). The forward primer is P53-C1: 5'-AGC TAA TGT GAC TTC GCA TTG AAC AAA-3', and the reverse primer is P53-C2: 5'-TCG ATA AAC ATT GGC TAC GGC GAT TGT. These primers were prepared by Integrated DNA Technologies. The deletion should produce a 4.0 kbp product, while the wild type allele should produce a 7.3 kbp product. We used i-MAX™ II from iNtRON Biotechnology for the long distance genomic PCRs.

Immuno-fluorescence and transmission electron microscopy. For immuno-fluorescence microscopy, larval tissues were fixed in a phosphate buffered solution containing freshly prepared paraformaldehyde (2% final concentration), washed, blocked and incubated with antibodies as described.[46] We used a previously characterized isoform-specific guinea pig antiserum[6] at 1/100 and an Alexa Fluor® 546-conjugated goat anti-guinea pig antibody (A11074, Molecular Probes) at 1/250 to demonstrate the loss of Nopp140-RGG in RNAi-expressing larvae. To demonstrate apoptosis in imaginal wing discs, we used rabbit anti-cleaved Caspase-3 (Asp175) (#9661, Cell Signaling Technology) at 1/200. This particular antibody has been well described as a marker for Caspase-9-like DRONC activity in apoptotic *Drosophila* cells.[15] The secondary antibody was the Alexa Fluor® 488-conjugated goat anti-rabbit from Molecular Probes (A11034) at 1/250. Tissues were stained with DAPI

at 1 µg/mL in the final wash buffer and viewed with a Zeiss Axioskop equipped with a SPOT RT/SE CCD camera (Diagnostic Instruments).

Transmission electron microscopy of wild type and Nopp140-RNAi-expressing larval tissues was performed as described.[20] Diploid tissues (imaginal discs and brains) and polyploid tissues (mid-gut and Malpighian tubules) were hand isolated, fixed and flat-embedded separately so we could section and analyze one known tissue at a time. From Nopp140-RNAi-expressing larvae, we captured 16 images of polyploid cells and 20 images of diploid cells. About half as many images were captured from the same wild type tissues. We used a JEOL 100CX operating at 80 KV and a magnification of 16,000×. Negatives (8 × 10 cm) were scanned at 1200 dpi. Resulting positive images were prepared using Photoshop.

Immuno-blots. Third instar larval lysates were prepared by using small plastic pestles designed for Eppendorf tubes. Larvae were homogenized in 267 µL of Laemmli sample buffer to which we added 3 µL of 0.1 M PMSF dissolved in isopropanol, 15 µL of a protease inhibitor cocktail (P-8340, Sigma-Aldrich Corp.) and 15 µL of 2-mercaptoethanol. The homogenate was then sonicated by 5 bursts using a Branson Digital Sonifier; each burst was for 5 sec at 40% maximum power. The resulting lysates were centrifuged for 30 min. The supernatant was boiled for 5 min and re-centrifuged for an additional 30 min. Lysate proteins were resolved by standard SDS-PAGE and blotted to nitrocellulose using a Bio-Rad Trans-Blot semi-dry transfer cell. Blots were blocked with 5% non-fat dry milk in TTBS. We used rabbit antibodies against ribosomal proteins RpL34 (center) and RpL23A (C-terminus) (Abgent; catalog numbers AP13207c-ev20 and AP1939b, respectively) at 1/2000 in 5% non-fat dry milk. We used the 81E11 rabbit monoclonal antibody directed against phospho-JNK (Thr183/Tyr185; Cell Signaling Technologies, #4668) and a rabbit anti-Hid antibody that was kindly provided by Hyung Don Ryoo[34] at New York University Medical School diluted to 1/1000 in TTBS.

Mass spectroscopy. Proteins resolved on SDS-polyacrylamide gels were identified by mass spectroscopy at Louisiana State University's Pennington Biomedical Research Center. Briefly, 2 mm gel plugs were automatically excised using a ProteomeWorks spot cutter (Bio-Rad) and deposited in a 96-well plate. In-gel tryptic digestion was performed using an automated robotic workstation (MassPrep, Waters Corp.). Gel plugs were washed with NH_4HCO_3 and CH_3CN followed by reduction and alkylation using 10 mM DTT and 55 mM iodoacetamide, respectively. Proteins were cleaved by sequencing grade trypsin (150 ng/gel plug) at 37°C overnight. The peptide fragments were extracted with 2% CH_3CN, 1% HCOOH in water and directly analyzed using liquid chromatography (LC)–tandem mass spectrometry (MS/MS). The peptides from each digested band were separated and analyzed using a capillary LC system coupled online with a nanospray quadrupole time-of-flight (Q-TOF) MS (Waters Corp.) as described.[47] Tandem mass spectra were analyzed using the ProteinLynx Global Server 2.5 software (Waters Corp.) against a Swiss Prot database. The database search settings included one missed tryptic cleavage and fixed carbamidomethylation of cysteine residues.

Hemolymph phenoloxidase assays. Relative hemolymph phenoloxidase levels were determined using native gels and staining techniques with tyrosine as substrate as described previously.[26]

Metabolic labeling. Twenty third-instar larvae, either parental controls or progeny expressing RNAi to deplete Nopp140, were added to ~300 µL of Robb's A + B solution[49] in disposable plastic depression slides and gently torn open to expose internal tissues. Excess fluid was removed leaving approximately 50 µL to which we added 10 µL of EXPRE^{35}S^{35}S Protein Labeling Mix, [^{35}S]-EasyTag™ (Perkin-Elmer, NEG772002M, 10.0 mCi/ml). The depression slides were placed in a moist chamber, and the tissues were incubated for 30 min at room temperature. Tissues were then washed once with Robb's A + B solution. Lysates were prepared by adding 25 µL of a protease inhibitor cocktail (Sigma-Aldrich, P-8340), 445 µL of Laemmli sample buffer, 25 µL 2-mercaptoethanol and 5 µL 0.1 M PMSF dissolved in isopropanol. Tissues were homogenized in Eppendorf tubes with disposal plastic pestles, boiled for five minutes and centrifuged for one hour. Protein concentrations were determined in triplicate using a modified Lowry assay.[50] Absorbance values were determined using a Perkin-Elmer Lambda 3B spectrophotometer. To determine incorporated CPM, 200 µL of larval lysate was combined with 100 µL of ddH$_2$O, 100 µL BSA (2 mg/ml) and 80 µL 100% TCA (16.7% final concentration). Samples were mixed and incubated on ice for 30 min. Each sample was passed through a vacuum filter assembly (Sigma-Aldrich, Z290475) containing a Whatman 25 mm GFC glass microfiber filter which was then rinsed with cold 10% TCA and 100% EtOH. Filters were air-dried and placed separately into 10 mL of Scintiverse (TM) BD Cocktail (Fisher Scientific). CPM was determined using a Beckman LS 6000IC scintillation counter. Ratios of CPM per microgram of protein were determined for each sample. The entire experiment was repeated three times. We also verified the relative protein concentrations and CPM values for each sample by resolving lysate proteins on SDS-10% polyacrylamide gels; Coomassie blue staining verified the relative protein concentrations. The gels were dried and exposed to Kodak X-OMAT LS film; resulting autoradiograms verified the relative scintillation counts.

References

1. Meier UT. Comparison of the rat nucleolar protein Nopp140 with its yeast homologue SRP40. Differential phosphorylation in vertebrates and yeast. J Biol Chem 1996; 271:19376-84; PMID:8702624.

2. Isaac C, Yang Y, Meier UT. Nopp140 functions as a molecular link between the nucleolus and the coiled bodies. J Cell Biol 1998; 142:319-29; PMID:9679133; http://dx.doi.org/10.1083/jcb.142.2.319.

3. Yang Y, Isaac C, Wang C, Dragon F, Pogacic V, Meier UT. Conserved composition of mammalian box H/ACA and box C/D small nucleolar ribonucleoprotein particles and their interaction with the common factor Nopp140. Mol Biol Cell 2000; 11:567-77; PMID:10679015.

4. He F, DiMario P. Structure and function of Nopp140 and Treacle. In: Olson MOJ, ed. The Nucleolus, Protein Reviews. New York, NY: Springer, 2011:253-278.

5. Waggener JM, DiMario PJ. Two splice variants of Nopp140 in *Drosophila melanogaster.* Mol Biol Cell 2002; 13:362-81; PMID:11809845; http://dx.doi.org/10.1091/mbc.01-04-0162.

6. Cui Z, DiMario PJ. RNAi knockdown of Nopp140 induces *Minute*-like phenotypes in *Drosophila.* Mol Biol Cell 2007; 18:2179-91; PMID:17392509; http://dx.doi.org/10.1091/mbc.E07-01-0074.

7. Dixon MJ. Treacher Collins syndrome. Hum Mol Genet 1996; 5(Spec No):1391-6; PMID:8875242.

8. Trainor PA, Dixon J, Dixon MJ. Treacher Collins syndrome: etiology, pathogenesis and prevention. Eur J Hum Genet 2009; 17:275-83; PMID:19107148; http://dx.doi.org/10.1038/ejhg.2008.221.

9. Dixon J, Jones NC, Sandell LL, Jayasinghe SM, Crane J, Rey JP, et al. *Tcof1*/Treacle is required for neural crest cell formation and proliferation deficiencies that cause craniofacial abnormalities. Proc Natl Acad Sci U S A 2006; 103:13403-8; PMID:16938877; http://dx.doi.org/10.1073/pnas.0603730103.

10. Jones NC, Lynn ML, Gaudenz K, Sakai D, Aoto K, Rey JP, et al. Prevention of the neurocristopathy Treacher Collins syndrome through inhibition of p53 function. Nat Med 2008; 14:125-33; PMID:18246078; http://dx.doi.org/10.1038/nm1725.

11. Shiba T, Saigo K. Retrovirus-like particles containing RNA homologous to the transposable element *copia* in *Drosophila melanogaster.* Nature 1983; 302:119-24; PMID:6186922; http://dx.doi.org/10.1038/302119a0.

12. Strand DJ, McDonald JF. *Copia* is transcriptionally responsive to environmental stress. Nucleic Acids Res 1985; 13:4401-10; PMID:2409535; http://dx.doi.org/10.1093/nar/13.12.4401.

13. Gartner LP, Gartner RC. Nuclear inclusions: a study of aging in *Drosophila.* J Gerontol 1976; 31:396-404; PMID:178709; http://dx.doi.org/10.1093/geronj/31.4.396.

14. Tulin A, Stewart D, Spradling AC. The Drosophila heterochromatic gene encoding poly(ADP-ribose) polymerase (PARP) is required to modulate chromatin structure during development. Genes Dev 2002; 16:2108-19; PMID:12183365; http://dx.doi.org/10.1101/gad.1003902.

15. Fan Y, Bergmann A. The cleaved-Caspase-3 antibody is a marker of Caspase-9-like DRONC activity in *Drosophila.* Cell Death Differ 2010; 17:534-9; PMID:19960024; http://dx.doi.org/10.1038/cdd.2009.185.

16. Rong YS, Titen SW, Xie HB, Golic MM, Bastiani M, Bandyopadhyay P, et al. Targeted mutagenesis by homologous recombination in *D. melanogaster.* Genes Dev 2002; 16:1568-81; PMID:12080094; http://dx.doi.org/10.1101/gad.986602.

17. Jaklevic BR, Su TT. Relative contribution of DNA repair, cell cycle checkpoints, and cell death to survival after DNA damage in *Drosophila* larvae. Curr Biol 2004; 14:23-32; PMID:14711410; http://dx.doi.org/10.1016/j.cub.2003.12.032.

18. Wichmann A, Jaklevic B, Su TT. Ionizing radiation induces caspase-dependent but Chk2- and p53-independent cell death in *Drosophila melanogaster.* Proc Natl Acad Sci U S A 2006; 103:9952-7; PMID:16785441; http://dx.doi.org/10.1073/pnas.0510528103.

19. Wichmann A, Uyetake L, Su TT. E2F1 and E2F2 have opposite effects on radiation-induced p53-independent apoptosis in *Drosophila.* Dev Biol 2010; 346:80-9; PMID:20659447; http://dx.doi.org/10.1016/j.ydbio.2010.07.023.

20. Rosby R, Cui Z, Rogers E, deLivron MA, Robinson VL, DiMario PJ. Knockdown of the *Drosophila* GTPase nucleostemin 1 impairs large ribosomal subunit biogenesis, cell growth, and midgut precursor cell maintenance. Mol Biol Cell 2009; 20:4424-34; PMID:19710426; http://dx.doi.org/10.1091/mbc.E08-06-0592.

21. Chang YY, Neufeld TP. An Atg1/Atg13 complex with multiple roles in TOR-mediated autophagy regulation. Mol Biol Cell 2009; 20:2004-14; PMID:19225150; http://dx.doi.org/10.1091/mbc.E08-12-1250.

22. Wu H, Wang MC, Bohmann D. JNK protects Drosophila from oxidative stress by transcriptionally activating autophagy. Mech Dev 2009; 126:624-37; PMID:19540338; http://dx.doi.org/10.1016/j.mod.2009.06.1082.

23. Neufeld TP. Autophagy and cell growth--the yin and yang of nutrient responses. J Cell Sci 2012; 125:2359-68; PMID:22649254; http://dx.doi.org/10.1242/jcs.103333.

24. Tang H. Regulation and function of the melanization reaction in *Drosophila.* Fly (Austin) 2009; 3:105-11; PMID:19164947; http://dx.doi.org/10.4161/fly.3.1.7747.

25. Roberts DB, Wolfe J, Akam ME. The developmental profiles of two major haemolymph proteins from *Drosophila melanogaster.* J Insect Physiol 1977; 23:871-8; PMID:415089; http://dx.doi.org/10.1016/0022-1910(77)90013-0.

26. Asano T, Takebuchi K. Identification of the gene encoding pro-phenoloxidase A($_3$) in the fruitfly, *Drosophila melanogaster.* Insect Mol Biol 2009; 18:223-32; PMID:19141111; http://dx.doi.org/10.1111/j.1365-2583.2008.00858.x.

27. Lin A. Activation of the JNK signaling pathway: breaking the brake on apoptosis. Bioessays 2003; 25:17-24; PMID:12508278; http://dx.doi.org/10.1002/bies.10204.

28. Weston CR, Davis RJ. The JNK signal transduction pathway. Curr Opin Cell Biol 2007; 19:142-9; PMID:17303404; http://dx.doi.org/10.1016/j.ceb.2007.02.001.

29. Bilak A, Su TT. Regulation of Drosophila melanogaster pro-apoptotic gene hid. Apoptosis 2009; 14:943-9; PMID:19554451; http://dx.doi.org/10.1007/s10495-009-0374-2.

30. Juhász G, Puskás LG, Komonyi O, Érdi B, Maróy P, Neufeld TP, et al. Gene expression profiling identifies FKBP39 as an inhibitor of autophagy in larval *Drosophila* fat body. Cell Death Differ 2007; 14:1181-90; PMID:17363962; http://dx.doi.org/10.1038/sj.cdd.4402123.

31. Chang YY, Neufeld TP. Autophagy takes flight in *Drosophila.* FEBS Lett 2010; 584:1342-9; PMID:20079355; http://dx.doi.org/10.1016/j.febslet.2010.01.006.

32. Bidla G, Dushay MS, Theopold U. Crystal cell rupture after injury in *Drosophila* requires the JNK pathway, small GTPases and the TNF homolog Eiger. J Cell Sci 2007; 120:1209-15; PMID:17356067; http://dx.doi.org/10.1242/jcs.03420.

33. McNamee LM, Brodsky MH. p53-independent apoptosis limits DNA damage-induced aneuploidy. Genetics 2009; 182:423-35; PMID:19364807; http://dx.doi.org/10.1534/genetics.109.102327.

34. Ryoo HD, Gorenc T, Steller H. Apoptotic cells can induce compensatory cell proliferation through the JNK and the Wingless signaling pathways. Dev Cell 2004; 7:491-501; PMID:15469838; http://dx.doi.org/10.1016/j.devcel.2004.08.019.

35. Minakhina S, Steward R. Melanotic mutants in *Drosophila*: pathways and phenotypes. Genetics 2006; 174:253-63; PMID:16816412; http://dx.doi.org/10.1534/genetics.106.061978.

36. Mayer C, Grummt I. Cellular stress and nucleolar function. Cell Cycle 2005; 4:1036-8; PMID:16205120; http://dx.doi.org/10.4161/cc.4.8.1925.

37. Tollini LA, Frum RA, Zhang Y. The role of the nucleolus in the stress response. In: Olson MOJ, ed. The Nucleolus, Protein Reviews. New York, NY: Springer, 2011:281-299.

38. Gowda PS, Zhou F, Chadwell LV, McEwen DG. p53 binding prevents phosphatase-mediated inactivation of diphosphorylated c-Jun N-terminal kinase. J Biol Chem 2012; 287:17554-67; PMID:22467874; http://dx.doi.org/10.1074/jbc.M111.319277.

39. Luo X, Puig O, Hyun J, Bohmann D, Jasper H. Foxo and Fos regulate the decision between cell death and survival in response to UV irradiation. EMBO J 2007; 26:380-90; PMID:17183370; http://dx.doi.org/10.1038/sj.emboj.7601484.

40. Moreno E, Basler K, Morata G. Cells compete for decapentaplegic survival factor to prevent apoptosis in *Drosophila* wing development. Nature 2002; 416:755-9; PMID:11961558; http://dx.doi.org/10.1038/416755a.

41. Marygold SJ, Roote J, Reuter G, Lambertsson A, Ashburner M, Millburn GH, et al. The ribosomal protein genes and *Minute* loci of *Drosophila melanogaster.* Genome Biol 2007; 8:R216; PMID:17927810; http://dx.doi.org/10.1186/gb-2007-8-10-r216.

42. Mayer C, Bierhoff H, Grummt I. The nucleolus as a stress sensor: JNK2 inactivates the transcription factor TIF-IA and down-regulates rRNA synthesis. Genes Dev 2005; 19:933-41; PMID:15805466; http://dx.doi.org/10.1101/gad.333205.

43. Yogev O, Saadon K, Anzi S, Inoue K, Shaulian E. DNA damage-dependent translocation of B23 and p19^ARF is regulated by the Jun N-terminal kinase pathway. Cancer Res 2008; 68:1398-406; PMID:18316603; http://dx.doi.org/10.1158/0008-5472.CAN-07-2865.

44. Mialon A, Thastrup J, Kallunki T, Mannermaa L, Westermarck J, Holmström TH. Identification of nucleolar effects in JNK-deficient cells. FEBS Lett 2008; 582:3145-51; PMID:18703060; http://dx.doi.org/10.1016/j.febslet.2008.08.004.

45. Haerry TE, Khalsa O, O'Connor MB, Wharton KA. Synergistic signaling by two BMP ligands through the SAX and TKV receptors controls wing growth and patterning in Drosophila. Development 1998; 125:3977-87; PMID:9735359.

46. de Cuevas M, Lee JK, Spradling AC. alpha-spectrin is required for germline cell division and differentiation in the *Drosophila* ovary. Development 1996; 122:3959-68; PMID:9012516.

47. Zvonic S, Lefevre M, Kilroy G, Floyd ZE, DeLany JP, Kheterpal I, et al. Secretome of primary cultures of human adipose-derived stem cells: modulation of serpins by adipogenesis. Mol Cell Proteomics 2007; 6:18-28; PMID:17018519; http://dx.doi.org/10.1074/mcp.M600217-MCP200.

48. Chintapalli VR, Wang J, Dow JAT. Using FlyAtlas to identify better *Drosophila melanogaster* models of human disease. Nat Genet 2007; 39:715-20; PMID:17534367; http://dx.doi.org/10.1038/ng2049.

49. Robb JA. Maintenance of imaginal discs of *Drosophila melanogaster* in chemically defined media. J Cell Biol 1969; 41:876-85; PMID:5768877; http://dx.doi.org/10.1083/jcb.41.3.876.

50. Peterson GL. Determination of total protein. Methods Enzymol 1983; 91:95-119; PMID:6855607; http://dx.doi.org/10.1016/S0076-6879(83)91014-5.